Functional characterization of LHT7's role in plant immunity

ZHUYUAN HU
Charlottesville, Virginia

Bachelor of Agriculture, Nanjing Agricultural University, Nanjing, 2021

A Dissertation presented to the Graduate Faculty
of the University of Virginia in Candidacy for the Degree of
Master of Science

Department of Biology

University of Virginia
May 2023

ABSTRACT

Plants are constantly exposed to microbes. To survive, they evolve mechanisms to receive microbes and prevent infection. Pattern Recognition Receptors (PRRs) localized at the plasma membrane detect Pathogen-Associated Molecular Patterns (PAMPs) produced by microbes. When PRRs detect PAMPs, they induce defense responses that suppress microbial growth, and hence, the infection. This type of defense is called PAMP-triggered immunity (PTI) and typically leads to changes in the composition of metabolites that inhibit microbial growth by suppressing the expression of microbial virulence factors (Zhang et al., 2022; Zhang et al., 2023).

Pathogenic bacteria usually colonize the leaf apoplast, the intercellular space surrounding photosynthetic cells within the leaf mesophyll. Once in the leaf apoplast, bacteria can take up and metabolize plant-made carbon and nitrogen-containing sugars and amino acids to support their growth (Farvardin et al., 2020). Recent studies show that when plants perceive PAMPs, the concentration of amino acids increases in the leaf apoplast, thus impacting microbial growth (Zhang et al., 2023). However, the mechanisms that regulate the amino acid concentration in apoplast during PTI are still poorly understood (Zhang et al., 2022).

Nitrogen is an essential nutrient for plants and is usually transported across tissues in its reduced form as amino acids. The transport of amino acids between different cells and tissues requires amino acids transporter protein localized at cell membranes (Tegeder et al., 2012; Somawala et al., 2018). The Lysine–Histidine-like Transporters (LHT) family is a class of amino acid transporter that belongs to the ATF (Amino acid Transporter Family) (Ortiz-

Lopez et al., 2000). The ATF superfamily contains six subfamilies: AAP (Amino Acid Permease), ProT (Proline Transporter), LHT, ANT1-like (Aromatic and Neutral amino acid Transporter), AUX/LAX (Auxin influx carriers), and GAT (Gama-Aminobutyric acid Transporter) (Tegeder et al., 2012). Some members within these families are well studied, and most of them have been confirmed to transport amino acids against a concentration gradient using a proton (H+) couple transport mechanism. To identify transporters that may contribute to modulating the concentration of amino acids in the leaf apoplast of *Arabidopsis thaliana*, I searched for H+ coupled amino acid transporters upregulated in response to PAMPs treatment (http://bar.utoronto.ca/). I found that *LHT1* and *LHT7* are highly induced in response to the PAMP flagellin-22 amino acids peptide (flg22), a canonical PAMP derived from gram-negative bacterial flagellin protein. Preliminary data produced in the Danna lab showed that *LHT7* loss-of-function mutant plants (*lht7*) are more susceptible to *Pseudomonas syringae* infections than wild-type plants. As *LHT7* is induced by flg22 and the *lht7* mutants are susceptible to infections, an in-depth characterization will advance our understanding of the role of amino acid transport in plant immunity. Therefore, the *LHT7*'s role in plant immunity during infection is the overarching question that drives my research. I hypothesize that the *LHT7* transporter contributes to the flg22-elicited changes in the concentration of amino acids that are needed to suppress *P. syringae* infections.

TABLE OF CONTENT

Background and Significance

Background

Overview of plant immunity

As the primary producer in nature, plants constitute the material basis for the survival of all living things and maintain material circulation and balance. How plants overcome the challenges posed by surrounding microbes remains an open question, given that they lack an immune system similar to that found in mammals. To understand plant immunity, researchers use *Arabidopsis thaliana* as a model plant to study the interactions between plants and microbes. *Arabidopsis* is a genetically tractable model plant of small size with a relatively short life cycle and self-pollinate, thus facilitating the characterization of genes and their functions (Krämer, 2015). Through long periods of interaction, bacteria and plants have undergone co-evolution and developed sophisticated mechanisms to combat each other (Jones and Dangl, 2006). For foliar bacterial pathogens, they tend to aggregate near trichomes at the leaf surface and penetrate the epidermis through stomata. After extensive multiplication within the leaf apoplast, visible disease-associated chlorosis appears (Melotto et al., 2008). However, plants have their own set of defenses against these pathogens. The cells of plants have receptors known as Pattern Recognition Receptors (PRRs) that monitor the invasion of pathogens. These PRRs are located on the cell surface and recognize specific Pathogen-Associated Molecular Patterns (PAMPs). For instance, the Leu-rich repeat transmembrane receptor kinase FLAGELLIN SENSITIVE-2 (FLS2) is crucial in identifying flagellin, a vital component of the bacterial flagellum (Chinchilla et al., 2006). PRRs usually comprise two domains: an extracellular leucine-rich repeat (LRR) domain and an intracellular kinase domain. To initiate the Pathogen-Triggered Immunity (PTI) signaling pathway, many PRRs require the assistance of a related protein called BRASSINOSTEROID INSENSITIVE 1-ASSOCIATED

KINASE 1 (BAK1) (Dodds et al., 2010). PTI is a low-level inducible immunity that can stop the initiation of apoplast colonization by non-adapted pathogens. However, bacterial pathogens employed a Type-3 Secretion System (T3SS) to deliver effector proteins (T3E) to the host cells. These host-adapted bacteria make full use of effectors to suppress PTI, which facilitates leaf colonization. If the plant expresses nucleotide-binding domain/leucine-rich repeat (NLR) cytoplasmic receptors to detect incoming T3E, they will activate ETI. More often than not, the onset of ETI triggers program cell death and the clearance of the attempted infection. Therefore, by combining PTI and ETI, plants can effectively suppress microbial infection. Both PAMPs and T3E evoke similar responses, such as the activation of NADPH oxidase activity (RBOHD), the production of Reactive Oxygen Species (ROS), and changes in defense-related hormone levels, among other responses (Pruitt et al., 2021; Dodds et al., 2010; Jones et al., 2006).

Virulence of *Pseudomonas syringae pv. tomato DC3000*

Various strains of gram-negative bacteria *Pseudomonas syringae* have been used as model pathogens to understand the interactions between plants and microbes since the 1980s. In 1991, researchers found *Pseudomonas syringae pv. tomato DC3000 (Pst)* is capable of causing diseases, not only in tomato but also in a variety of plant species, including *Arabidopsis thaliana* and *Nicotiana benthamiana,* two model plants that are commonly used in laboratories. This finding sparked extensive research into studying the mechanisms of how these species infect plants over the next two decades (Xin et al., 2013). In 2003, Its complete genome was sequenced, and people found it consists of a circular chromosome and two plasmids. *Pst* contains numerous genes that are responsible for acquiring nutrients and facilitating infection in plants. More than 12% of the genes are dedicated to regulation, which suggests that the organism

must be able to adapt quickly to different environments during both epiphytic growth and pathogenesis (Buell et al., 2003). The *Pst* genome also contains genes that encode types I, II, III, IV, V, and VI and twin-arginine transporter (Tat) secretion systems (Cunnac et al., 2009; Lindeberg et al., 2008). Among these secretion systems, Type-3 Secretion System (T3SS) is especially important because of its virulence. The T3SS is encoded by the *hrp* (hypersensitive response and pathogenicity) and *hrc* (*hrp* conserved) genes and assembles a syringe-like supramolecular complex on the bacterial envelope. It is a key virulence factor of *Pst DC3000* and many other gram-negative bacterial pathogens of plants and animals (Buttner et al., 2009; Galan et al., 1999). This system delivers effector proteins (T3E) into the plant cells which can suppress PTI. *Pst DC3000* can also synthesize the polyketide toxin coronatine, a non-host-specific polyketide toxin composed of two structural components, coronamic acid (CFA) and coronafacic acid (CMA), which mimic the plant hormone jasmonate (JA) in structure (Tang et al., 2006). Coronatine plays multiple roles in plant infection, such as the promotion of bacterial invasion through stomata, facilitation of bacterial growth and survival within plants, increased susceptibility to disease, and induction of disease symptoms (Xin et al., 2013). For example, when applied coronatine to plants, they would show chlorosis. However, the coronatine mutant would reduce the disease symptoms significantly (Bender et al., 1999; Brooks et al., 2005; Brooks et al., 2004). T3SS induction and coronatine synthesis are both energy-intensive processes. As a result, it is not unexpected that *Pst* would increase their expression of these processes only in the presence of plant hosts, rather than in a nutrient-rich medium (Aung et al., 2020).

The *Arabidopsis thaliana* and *Pseudomonas syringae* combination is a well-established model system for studying plant immunity and has greatly

6

contributed to our understanding of bacterial diseases in plants. However, we still lack a clear understanding of whether and how bacteria actively obtain nutrients from host plants. Furthermore, most research is conducted under artificial bacterial infection conditions, which can lead to overestimation or underestimation of virulence factors. Although this model system has generated many exciting concepts, it is essential to find ways to translate this basic understanding into practical solutions for field applications (Xin et al., 2013).

Amino acid transporters in plant immunity

Nitrogen (N) is a crucial microelement that is the most limiting factor for plant growth and development. Plants primarily absorb inorganic nitrogen sources, such as nitrates and ammonium, through their roots. However, they can also absorb organic nitrogen sources, such as amino acids (Näsholm et al., 2009). Plants can convert inorganic nitrogen into amino acids through metabolic processes occurring in leaves or roots. In most plants, the amino acids produced in leaves or derived from roots are transported through the phloem to the sink organs. This process is crucial for the distribution of nutrients throughout the plant, ensuring that all tissues and organs of the plant have access to the necessary nitrogen (Frommer et al., 1993; Tegeder et al., 2018). The identification of the first plant amino acid transporters was achieved through the functional complementation of yeast mutants (Hsu et al., 1993; Frommer et al., 1995). With the development of bioinformatics analysis and whole genome sequencing of various plant species, additional amino acid transporters were subsequently discovered (Schwacke et al., 2003). Although these transporters belong to different families, they exhibit several standard features, including broad substrate selectivity and expression patterns (Yang et al., 2020). For instance, the expression level of *AAP1* transporter was higher in

the mature leaves of potato than in other sink organs such as roots and immature leaves (Koch et al., 2003). The expression of the *ANT1* transporters can be detected in every tissue and organ of Arabidopsis plants, but the high level of mRNA is only detected in flowers and cauline leaves (Chen et al., 2001).

Previous studies have shown that several amino acid transporters, such as *LHT1* and *AAP1* in Arabidopsis, can directly uptake amino acids from the external medium (Hirner et al., 2006; Lee et al., 2007; Agorsor et al., 2023). These findings primarily rely on observations of mutant defects, where certain amino acid transporters exhibit slow growth and reduce amino acid uptake on a culture medium where amino acids are the sole nitrogen source. However, most of these studies used agar medium or nutrient solutions with appropriate pH and concentration (Svennerstam et al., 2011; Perchlik et al., 2014). Therefore, we still lack an understanding of how these transporters can uptake amino acids directly from the soil, and their contribution to the plant's nitrogen resource requirements is still limited (Yang et al., 2020). Amino acids originating from the roots are transported to the shoots through the xylem. During this long-distance transport, some amino acids can move from the xylem to the phloem, and subsequently provide nitrogen directly to the sink tissues (Tegeder et al., 2018). The amino acids synthesis in mesophyll cells can be transported to the phloem either through a symplastic or an apoplastic pathway. The specific pathway utilized depends on the presence or absence of plasmodesmata between companion cells and phloem parenchyma, as well as their frequency (Tegeder, 2014). In Arabidopsis and most dicotyledonous crops, amino acids synthesized in the mesophyll cells leak into the leaf apoplast from where they are either reclaimed by local photosynthetic cells or taken up by the phloem companion cells for long-distance translocation. This phloem loading apoplastic

route offers opportunities for biotrophic pathogens to gain access to readily usable organic carbon and nitrogen to sustain microbial growth and infections. Upon entering the leaf apoplast, biotrophic microbes rely on plant metabolites for their nutrition. Therefore, the interaction between microbes and plants is tightly linked to the availability and flux of nutrients in the leaf apoplast. The transport of amino acids across membranes is tightly controlled by amino acid transporters. Several lines of evidence indicate that the availability of the amino acid near the infection site can decide the success or failure of the bacterial pathogen *Pseudomonas syringae* to establish infections. For instance, exposing plants to PAMPs like flg22 or the 26-aa long Elongation Factor-Tu synthetic peptide (elf26) induces changes in the concentrations of leaf apoplastic metabolites and plants' resistance to *P. syringae* (Zhang et al., 2022).

Transcriptomic analysis of plant interacting with biotrophic microbes has shown that the accumulation of mRNA for genes encoding amino acid transporters is altered during infection (Fig 1). Notably, the expression of the amino acid transporters *CAT1*, *LHT1*, and *LHT7* increased significantly when challenged with
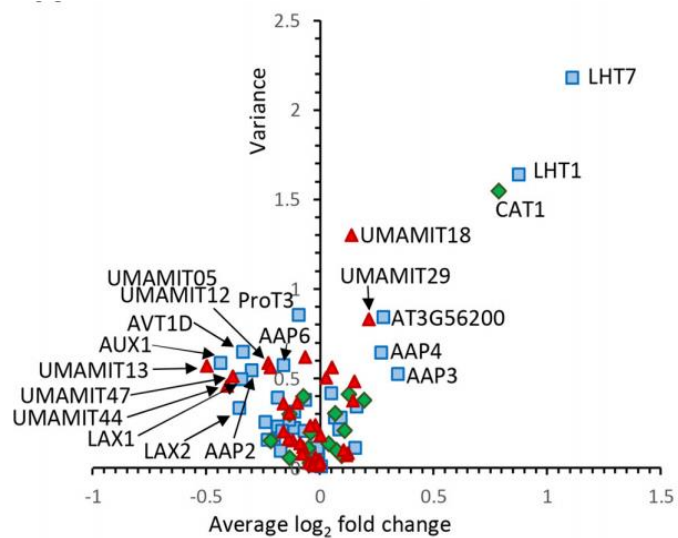

Figure 1. Relationship between variance and average of expression change for the Arabidopsis amino acid transporter family genes in plants infected by various pathogens. Labeled genes are among the ones responding to most to the infections. Blue squares: Amino Acid Auxin Permease (AAAP) family genes, Red triangles: Amino acid, Polyamine and organocation (APC) family genes; Green diamonds: Usually Many Amino acids Move In and out Transporter (UMAMIT) family genes.

most biotrophic pathogens (Sonawala et al., 2018). While the role of *CAT1* and *LHT1* in transport and immunity has been partially addressed in previous studies, the role of *LHT7* in plant immunity remains unexplored.

Preliminary Data

The metabolite composition of the leaf apoplast of plants is similar to that of the conditioned liquid medium where Arabidopsis seedlings are grown in sterile conditions. As seedlings germinate and grow in the liquid medium, they exude apoplastic metabolites into the liquid (i.e., seedling exudates). Previous studies show that the onset of PTI is accompanied by changes in organic acids in the liquid exudates of seedlings (Anderson et al., 2014). The concentrations of amino acids also change during the onset of PTI, and the changes contribute to plant immunity (Zhang et al., 2022; Zhang et al., 2023). The total amino acid concentration increased significantly within the first 4 h, then decreased and remained low from 12 h to 24 h after flg22 treatment (Fig 2A). Uptake assays using radiolabeled amino acids show that amino acid uptake activity is inhibited by flg22 within the 1 h post-elicitation but increased at later time points (Zhang, 2022a). These data suggest that the change in amino acids
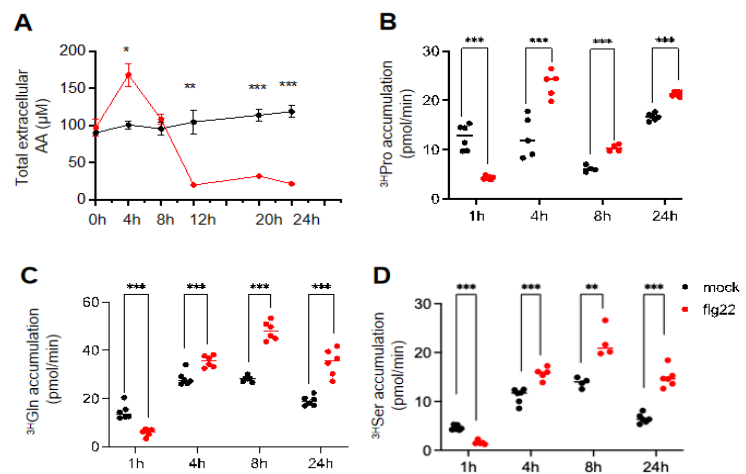

Figure 2. **MAMP perception induces changes in amino acid transport activity that modulate extracellular AA concentrations.** (**A**) Mean ± SEM (n=3) of total AA concentrations in the liquid exudates of mock- (black) or flg22-treated (red) wild-type seedlings. (**B**) ^{3H}Pro, (**C**) ^{3H}Gln, and (**D**) ^{3H}Ser) uptake rates of wild-type seedlings pre-treated with water (black) or flg22 (red) for 1 h, 4 h, 8 h, or 24 h prior to assessing the uptake activity. n=6 replicates of ten seedlings per point. Data analysis: t-test (A); Welch t-test (B, C, D,). (*), (**), and (***) indicate statistically significant differences at p-values of <0.05 , <0.01, and <0.001, respectively.

concentration after perception of PTI depends on the activity of amino acid transporters. Gene expression analysis of flg22-treated seedlings showed that flg22 induces the expression of *LHT7*

and several other amino acid transporters that take up amino acids into the cells upstream a concentration gradient by co-transporting protons that are present at a higher concentration outside the cells (Fig 3). All these AA/H+ co-transporters have been previously studied, except *LHT7*. Importantly, loss-of-function mutations in *LHT7* have an enhanced susceptibility phenotype when inoculated with the

Figure 3. Relative expression of AA/H+ symporters in wild-type seedlings 8 h post flg22 treatment. mRNA levels were assessed with nanoString® hybridizations and analyzed with the nSolver® software. One-sample t-test data analysis. Total RNA samples were obtained from fifteen 10-day-old seedlings 8 h post flg22 treatment from three independent experiments.

pathogenic strains *Pst* DC3000 or *Psm* ES4326 (Fig 4). These data suggest that *LHT7* plays a positive role in plant immunity. The intracellular signaling molecule salicylic acid (SA) plays a crucial role in plant defense against *P. syringae* (Wildermuth et al., 2001). As shown in Figure 4, the enhanced susceptibility of the SA biosynthesis mutant *sid2* is additive to the enhanced susceptibility of the *lht7* mutant, suggesting that LHT7's role in plant immunity is independent of salicylic acid.
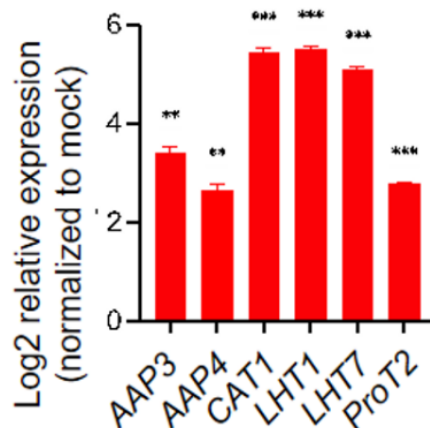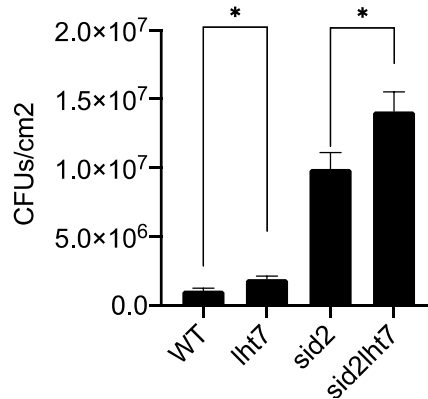

Fig 4. Knocking out LHT7 impairs defense response. 6-week-old plants are used for infection assay. *Psm ES4326* (OD=0.0002) is used for infiltration infection. CFUs in infected leaves are counted 48 hours after infection.

Significance

As the human population grows, the demand for food increases dramatically. Previous studies show that about 12% of crops are lost to microbial infections every year (Chakraborty et al., 2011). Understanding the relationship between the plant immune system and pathogens is significant in helping people find a way to develop better crops. As the most basic and ubiquitous defense pathway, PTI provides plants with a powerful tool against microbial invasion. The Danna lab, and a few others, are contributing evidence suggesting an essential role for amino acid transporters in modulating the availability of plant-made amino acids to invading bacteria (Ortiz-Lopez et al., 2000). Understanding *LHT7* contributions to immunity will help build a more complete model of plant defense.

Research Objectives

As amino acid transporters are responsible for importing and exporting amino acids, it is crucial to comprehend their role in plant immunity. *LHT7* is one of the genes that is highly induced during the PTI. My research aimed to define the tissue-specific and subcellular localization of *LHT7*'s and employ loss-of-function and gain-of-function lines to investigate its significance in plant immunity.

Results

Generate the tissue-specific expression line of *LHT7*

Tissue-specific expression of *LHT7* will help determine its physiological function. GUS (β-glucuronidase) reporters are well suited to visualize tissue and cell-specific promoter's activity. The GUS reporter system consists of the *uidA* gene that encodes the β-glucuronidase enzyme. This enzyme can react with the synthetic substrate X-Gluc and produce a stable blue precipitate that

can be visualized under the microscope (Blanco et al., 1982; Jefferson et al., 1986). I cloned the native promotor of *LHT7* upstream of *uidA* using Gibson recombination cloning and transferred the construct to Arabidopsis plants via Agrobacterium transformation of immature flowers (Deblaere et al., 1985; Clough S.J. and Bent A., 1998). Transgenic lines containing *pLHT7::uidA* will reveal the tissue-specific expression of *LHT7* under various conditions, such as defense elicitation with flg22, and infections with various virulent and non-virulence *P. syringae* strains. Figure 5 shows results obtained from the colony PCR after transforming Agrobacterium tumefaciens with a binary vector containing *pLHT7::uidA*: lanes #1 and #4 used Agrobacterium which contains *pLHT7::uidA* as the template. I used WT genomic DNA and the parental plasmid of the GUS reporter as the positive control. The product's size for the *LHT7* promoter should be 993 bp and 475 bp for the *uidA* ORF. The result shows that the construct was correctly assembled and transformed into Agrobacterium successfully (Fig 5).
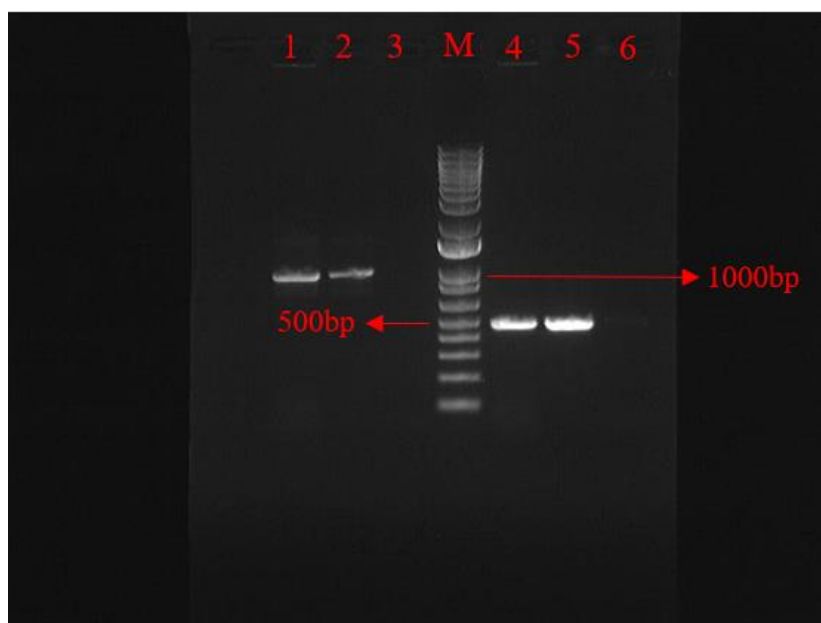

Fig 5. Detection of *pLHT7-GUS* in Agrobacterium. M: DNA Marker 1kb plus; 1&4: Transformed Agrobacterium; 2: WT as the template; 5: GUS parental plasmid; 3&6: Non-transformed Agrobacterium.

One positive Agrobacterium colony was used for overnight culture and the subsequent infection of immature flowers via floral dipping. Seeds from these T0 plants have been harvested and should be ready for germination tests on MS plates supplemented with Kanamycin to select seedlings that received the *pLHT7::uidA* containing T-DNA from the binary vector. Upon GUS staining, the blue precipitate produced by these transgenic plants will reveal the tissue specific expression driven by the *LHT7* promoter.

Define the *LHT7* subcellular localization.

Defining the subcellular localization of *LHT7* is necessary to predict its transport function. To assess the subcellular localization of LHT7 in *Arabidopsis thaliana* plants, I used Gibson cloning to create N- and C-terminal constructs containing the *LHT7* native promoter and the entire length of *LHT7* gDNA fused to the red fluorescent protein (mCherry). The gel images depict the Agrobacterium colony PCR results of these two constructs (Fig 6 and Fig 7). The identical sets of primers (Table 1) were utilized to detect *LHT7* native promoter, *LHT7* gDNA (that contains introns), and mCherry, each theoretically comprising 994bp, 1488bp, and 711bp, respectively. The agarose gel electrophoresis images revealed the successful PCR amplification of products of the correct size that I used for Gibson Assembly cloning reactions. Following this analysis, I used positive Agrobacterium clones to transform Arabidopsis plants via the floral dipping method. I have collected seeds from T0 plants. These T1 seeds will be germinated on MS agar plates with kanamycin to select seedlings that received the T-DNA containing *LHT7p::gLHT7*-mCherry and *LHT7p::*mCherry-*gLHT7*. Once positive transgenic lines are identified, further experiments should be performed to test if the localization of LHT7 was correctly reported by these mCherry fusions. In future experiments, Arabidopsis lines expressing *LHT7p::gLHT7*-mCherry and *LHT7p::*mCherry-*gLHT7* should be crossed with

lht7 mutants to test if the tagged LHT7 protein rescues the enhanced susceptibility phenotype of the mutants.

In case the native *LHT7* promoter produces low expression and does not allow for mCherry detection, I used Gateway to clone the gDNA fragment of *LHT7* fused to mCherry (C terminal fusion) under the control of the high expression constitutive promoter CaMV35S. This will allow high *LHT7*-mCherry expression that could facilitate the imaging of LHT7. After obtaining the construct, I transformed Arabidopsis plants and collected seeds, which were then screened on MS agar plates. Upon identifying transgenic lines (kanamycin-resistant seedlings), I extracted genomic DNA from the plants and used PCR primers to detect the mCherry ORF and thus verify the successful transformation of plants. The results demonstrated the presence of mCherry in the recovered plants (Fig 8). Subsequently, T2 seeds were collected and screened again on MS-kanamycin petri dishes. To confirm successful transcription, RNA was extracted from T2 seedlings and cDNA was synthesized and used as template in PCR reactions. Using primers that anneal on one *LHT7* exon and the mCherry ORF, which had a theoretical size of 1389bp, I demonstrated that *LHT7*-mCherry fusion is expressed in the seedlings (Fig 9). Then, I used 10-day-old seedlings to image LHT7 localization with a Leica confocal microscope (Leica STELLARIS 8). I used Arabidopsis transgenic plants expressing pm-rb *CD3-1008*, a well-established plasma membrane marker (mCherry) as a positive control for mCherry imaging. The expression of the plasma membrane maker is also controlled by the strong and constitutive CaMV35S promoter (Nelson et al., 2007). Wild-type Arabidopsis seedlings served as the negative control in the experiment, and the same settings were used to image all genotypes. The results revealed that the positive control exhibited a sharp and intense signal at the plasma membrane of every cell, while the wild-type plants

did not show any signals. However, the *35S::gLHT7-mCherry* transgenic line exhibited weak signals in foci that do not align with the plasma membrane. In future experiments, the Agrobacterium strain harboring this construct could be used to co-infiltrate Nicothiana bentamiana leaves with other Agrobacterium strains harboring GFP fusion of well-defined organelle markers. Colocalization of GFP markers and mCherry will define the subcellular localization of LHT7 (Kapila et al., 1997).
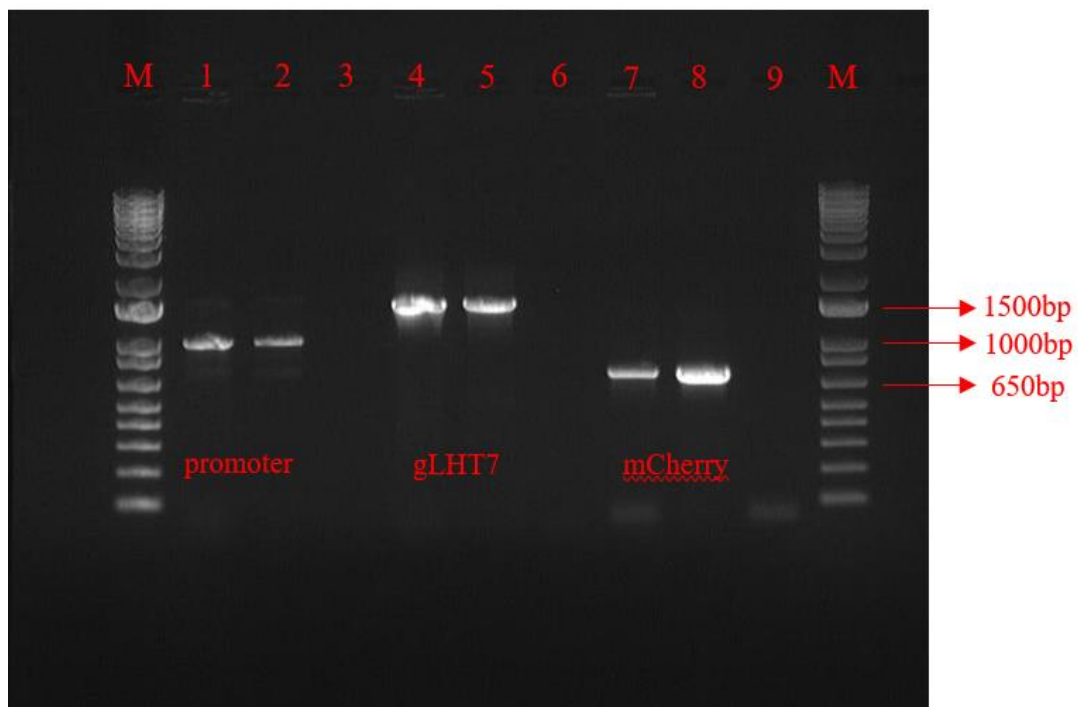

Fig 6. Detection of *pLHT7-gLHT7-mCherry* in Agrobacterium. M: DNA Marker 1kb plus; 1, 4&7: Transformed Agrobacterium; 2&5: WT as the template; 8: mCherry parental plasmid; 3, 6&9: Non-transformed Agrobacterium.

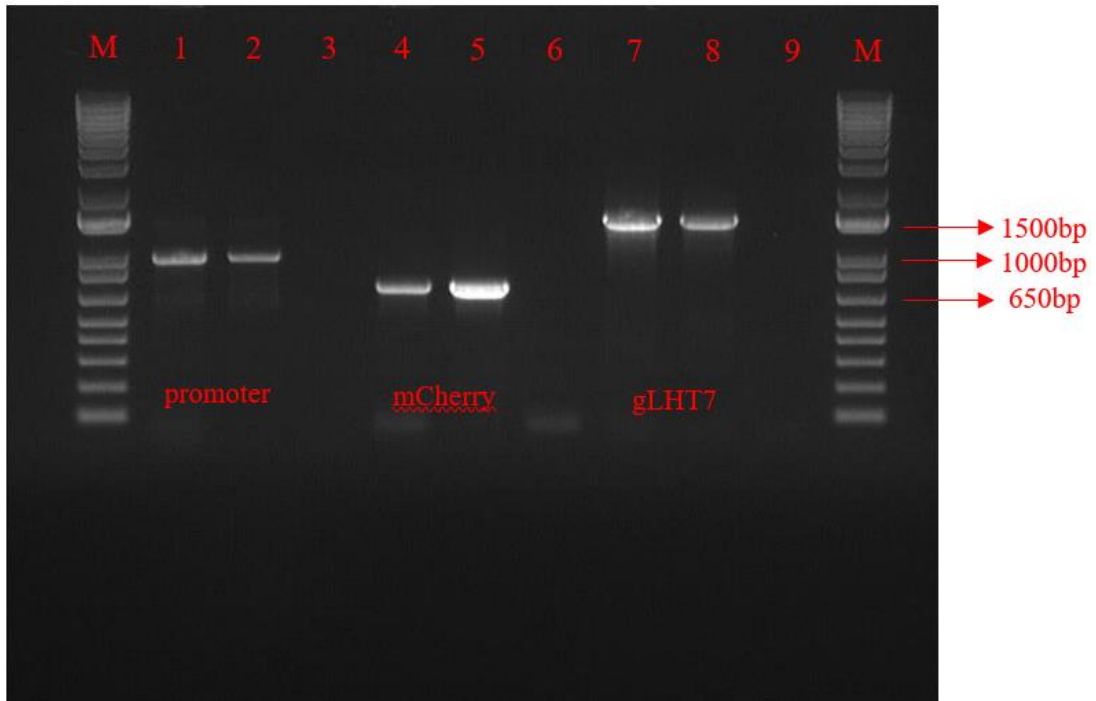**Fig 7. Detection of *pLHT7-mCherry-gLHT7* in Agrobacterium.** M: DNA Marker 1kb plus; 1, 4&7: Transformed Agrobacterium; 2&8: WT as the template; 5: mCherry parental plasmid; 3, 6&9: Non-transformed Agrobacterium.
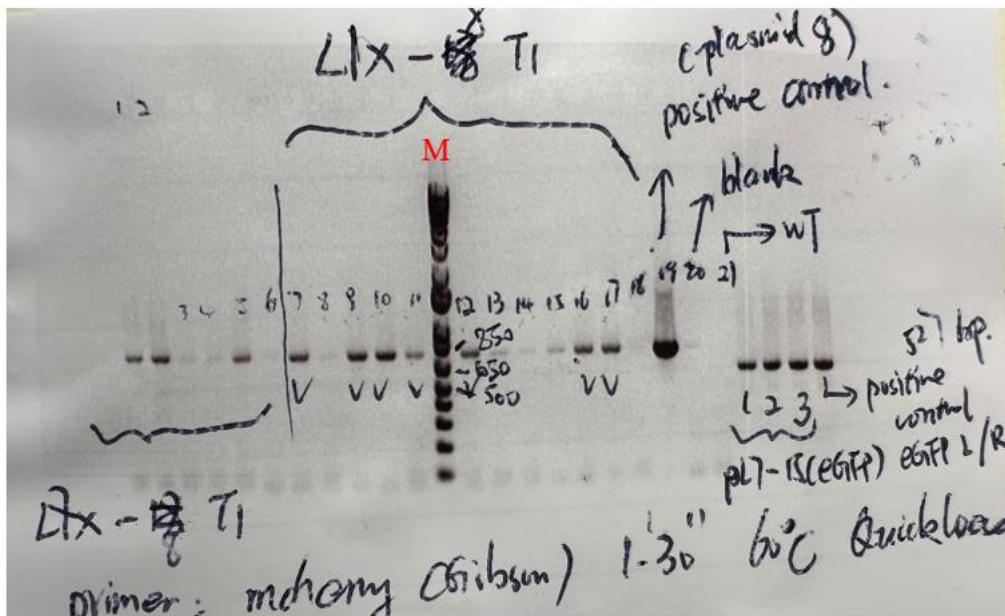

Fig 8. Genotyping of *35S::gDNA of LHT7 –mCherry* T1 plants. M: DNA Marker 1kb plus; 1, 2, 3, 4, 5&6: 35S::gDNA of *LHT7 –mCherry* transgenic T1 plants; 19: mCherry parental plasmid; 21: WT genomic DNA as the template
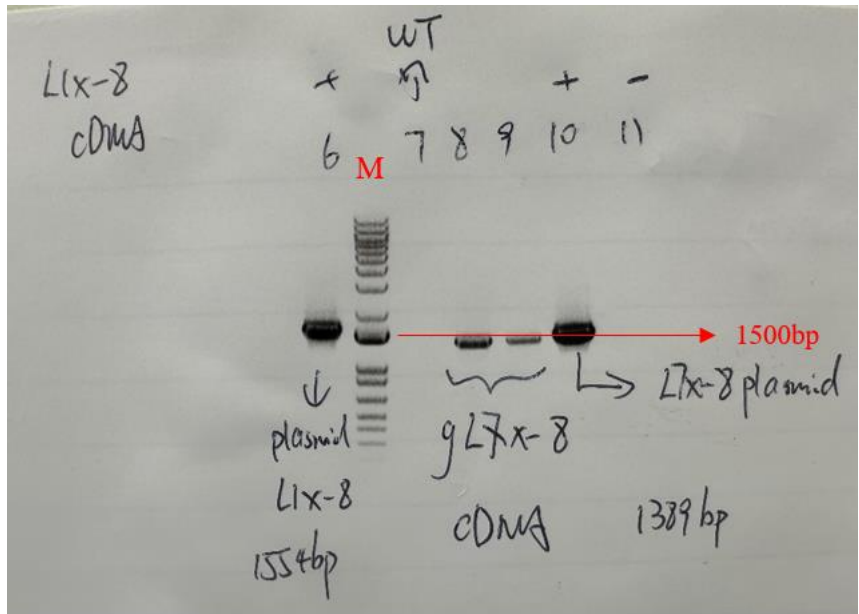
Fig 9. Detection of cDNA of *LHT7* and mCherry in T2 plants. M: DNA Marker 1kb plus; 8&9: cDNA of *LHT7* – mCherry extracted from T2 plants; 7: WT genomic DNA as the template; 10: 35S::gDNA of LHT7 –mCherry
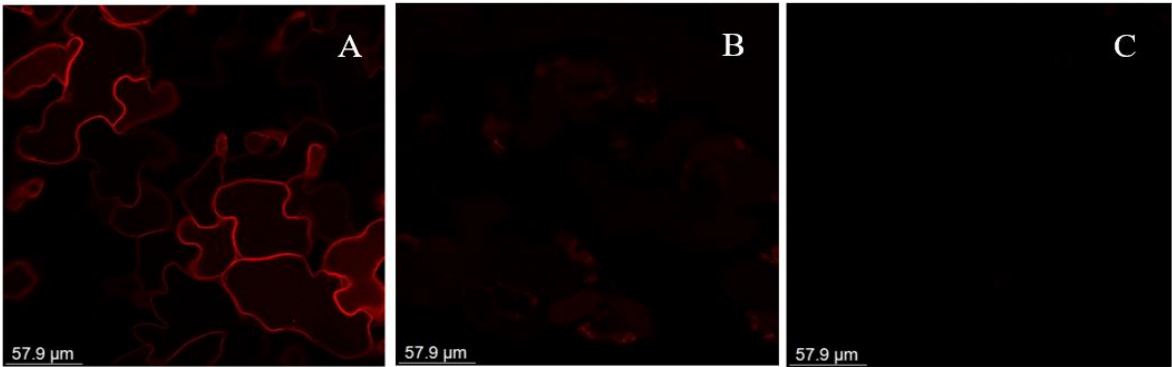

Fig 10. Localization of mCherry-fused gLHT7. The mCherry fluorescence signal is detected in the transgenic line *35S::gDNA of LHT7-mCherry* under the control of the 35S promoter. A. pm-rb *CD3-1008* transgenic line; B. *35S::gDNA of LHT7-mCherry* transgenic line; C. WT

Generate gain-of-function transgenic lines

To generate gain-of-function mutants, I used Gateway to clone the genomic DNA of *LHT7* (g*LHT7*) under the control of the Cassava Vein Mosaic Virus (CsVMV) promotor, a strong promotor that constitutively and ectopically expresses *LHT7* to similar levels in all plant tissues. The transgenic lines were confirmed via PCR genotyping (Fig 11). Before the infection assay, I assessed the expression level of *LHT7* to ensure they were overexpressed (Fig 12). Then, I used two loss-of-function insertional lines (SALK_027033 and SALK_043012), the gain-of-function mutants (CsVMV::gDNA of *LHT7*), and wild-type plants to do the plant bacterial infection assay. In this study, I used both *Pseudomonas syringae* pv. *maculicola* ES4326 (*Psm*) and *Pseudomonas syringae* pv *tomato* DC3000 (*Pst*) to inoculate the plant leaves. After counting the CFU, the result shows that there is no significant difference among the phenotypes (Fig 13).

Although constitutive ectopic gene expression provides a powerful tool for gene functional studies, the resulting ubiquitous expression may lead to lethality or pleiotropic defects unrelated to LHT7's function (Tegeder et al., 2012). To circumvent this problem, I generated estradiol-inducible constructs derived from the *pMDC7* plasmid containing an estradiol receptor and the estradiol inducible promoter. For this, I used Gateway and Gibson cloning to have *LHT7*'s CDS (c*LHT7*) or genomic (g*LHT7*) sequences downstream of the estradiol-inducible promoter. The results demonstrate that the constructs were successfully cloned and transformed into Agrobacterium (Fig 15 and Fig 16). In addition, I transformed Agrobacterium with the parental *pMDC7*-mCherry construct to serve as a negative control to use in future experiments. Upon exposing transgenic seedlings to estradiol, the fluorescence signal is expected to increase.
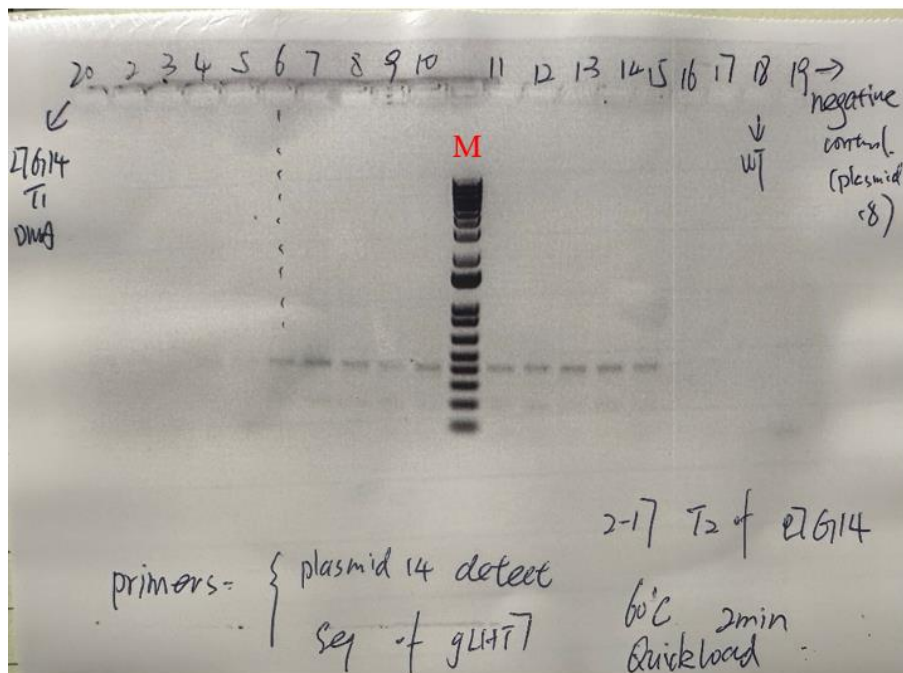
Fig 11. Genotyping of CsVMV::gDNA of *LHT7* T2 plants. M: DNA Marker 1kb plus; 2, 3, 4, 5, 6, 7, 8, 9, 10, 11, 12, 13, 14, 15, 16&17: CsVMV::gDNA of *LHT7* transgenic T2 plants genomic DNA; 18: WT genomic DNA as the template; 19: Blank
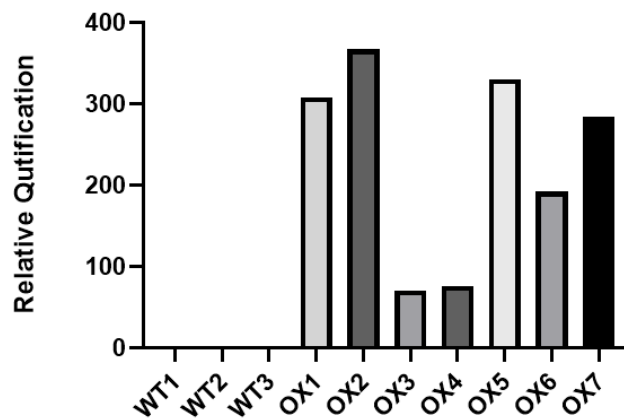

Fig 12. Transcriptional levels of *LHT7* in wild-type and CsVMV::gDNA of *LHT7* transgenic line. Relative Quantification Normalized to *ACT2*. The unpaired t-test is used.
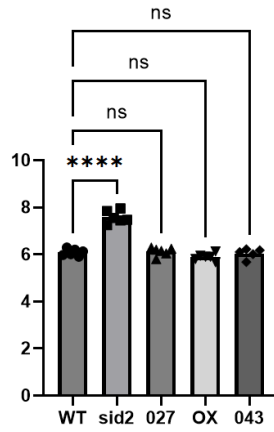
Fig 13. Infection assays among different phenotypes. 6-week-old plants are used for infection assay. *Psm ES4326* (OD=0.0002) is used for infiltration infection. CFUs in infected leaves are counted 48 hours after infection.

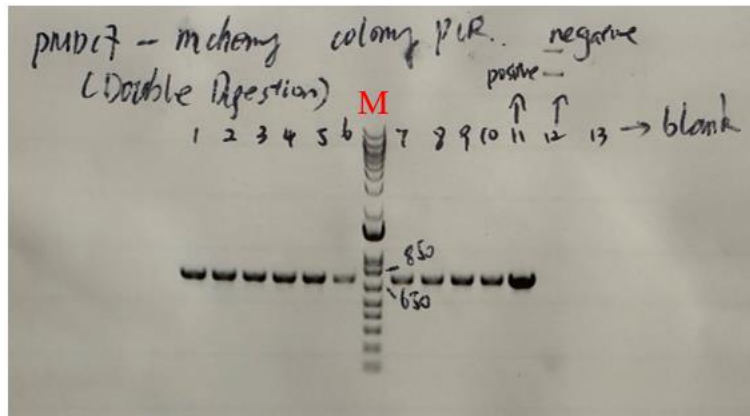**Fig 14. Detection of *pMDC7-mCherry* in Agrobacterium.** M: DNA Marker 1kb plus; 1, 2, 3, 4, 5, 6, 7, 8, 9&10: Transformed Agrobacterium; 11: mCherry parental plasmid as positive control; 12: Non-transformed Agrobacterium; 13: Blank.
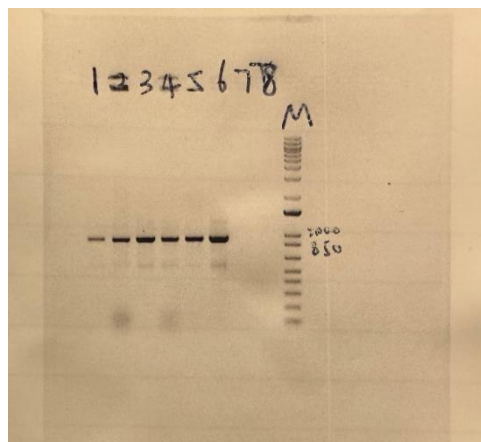

Fig 15. Detection of *pMDC7-CDS* of LHT7 in Agrobacterium. M: DNA Marker 1kb plus; 1, 2, 3, 4, 5&6: Transformed Agrobacterium; 7: Non-transformed Agrobacterium; 8: Blank.
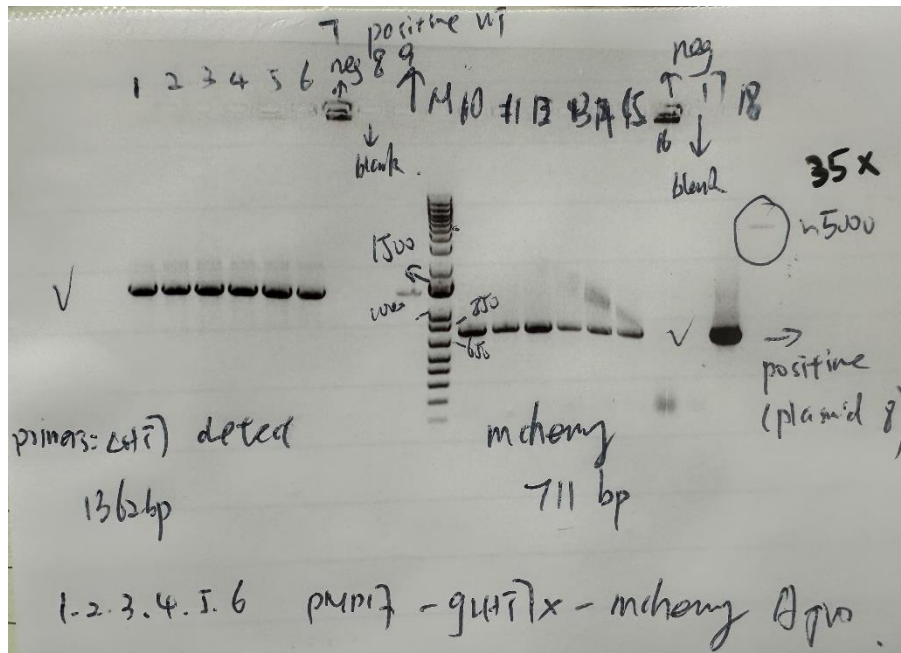
Fig 16. Detection of *pMDC7-gLHT7-mCherry* in Agrobacterium. M: DNA Marker 1kb plus; 1, 2, 3, 4, 5, 6, 10, 11, 12, 13, 14&15: Transformed Agrobacterium; 7&16: Non-transformed Agrobacterium; 9: WT genomic DNA as the template; 18: mCherry parental plasmid as positive control; 8&17: Blank

Discussion

The objective of this study was to investigate the tissue-specific and subcellular localization of *LHT7* and its role in plant immunity. Due to time constraints, I was only able to complete the cloning work and test the subcellular localization of *LHT7* and the cloning and testing of *LHT7* overexpression lines. The results suggest that *LHT7* does not localize to the plasma membrane. The foci observed in the mCherry imaging suggest that the signal localizes to an organelle. Further investigations are necessary to determine the precise localization and function of *LHT7* in the context of plant immunity. While the majority of the studied plant amino acid transporters localize to the plasma membrane, a few transporters are found in organelle membranes (Yang et al., 2020). Previous studies show that *LHT1*, a close homolog of *LHT7*, localizes to the plasma membrane (Hirner et al., 2006). I believe there are two primary factors that contributed to the low and foci signal intensity observed in the image

results. Firstly, the Agrobacterium-mediated transformation of plants produces insertions of the T-DNA carrying the construct of interest randomly into the plant genome. This could result in the T-DNA being inserted in a chromosome region where high gene expression is suppressed, leading to low mCherry signal. Secondly, the imaging process may also be affected by various issues, such as dirty glass slides, improperly fixed samples, and unhealthy plant seedlings. To improve the quality of the image results, the same construct could be used in Agrobacterium leaf infiltration for transient co-expression with organelle-specific markers in *N. benthamiana* leaves, where the T-DNA is not inserted into the plant genome and the constructs can be co-expressed transiently at high levels with other organelle marker tagged proteins. Additionally, protoplasts from the transgenic plants could be prepared to image the cells directly. This would eliminate the problem of having to image cells located deeper into the leaf tissue. This approach will allow us to avoid the challenges posed by thick plant tissue, uncleared samples, and weak signals.

Although preliminary data obtained by other graduate students show that loss-of-function mutants of *LHT7* are susceptible to bacterial infections, my result suggests there is no significant difference in colony forming units across wild type, loss-of-function, or gain-of-function genotypes. However, I cannot conclude that *LHT7* does not play a role in plant immunity. The enhanced susceptibility phenotype of *lht7* loss of function mutant, observed by two graduate students in previous years, was subtle but reproducible across multiple independent experiments. Thus, it is possible that factors related to the plant growth conditions that I used may have affected the data. For instance, growth conditions may have varied due to factors such as uneven light intensity, marginal temperature effects, and different wind speeds inside the growth incubator. Additionally, overexpression lines may result in unexpected

phenotypes or compensatory mechanisms that produce phenotypes unrelated to *LHT7* function. In this case, the alternative was to use estradiol-inducible constructs to transform Arabidopsis plants to test *LHT7*'s function at a specific time of the plant life cycle. In future experiments, Arabidopsis plants expressing these constructs in the *lht7* mutant background would allow to define if the induced but ectopic expression of LHT7 can rescue the enhanced susceptibility phenotype of *lht7*. Rescue experiments using LHT7 fusions to fluorescent proteins in the *lht7* mutant background would also allow to determine if the LHT7 imaging accurately reports the subcellular localization of the native LHT7 transporter.

Future Direction

Due to time constraints, I completed the cloning work but could not finish testing the transgenic plants that I obtained with the constructs that I generated. Some aspects of my original proposal will need to be addressed in future studies. Specifically, we need to determine the tissue-specific localization of LHT7 and its role in plant immunity. To achieve this, I have cloned *pLHT7::uidA* and introduced it into Arabidopsis, and I have collected the T1 seeds. It is necessary to screen these seeds on MS agar plates with kanamycin to identify transgenic plants and they will need to be imaged for tissue-specific localization of LHT7 under various conditions, including flg22 treatment. For the subcellular localization analysis, the *35S::gLHT7-mCherry* construct that I made could be co-infiltrated into *N. benthamiana* leaves along with a construct containing organelle-specific markers using Agroinfiltration of leaves. By observing the co-localization of LHT7 with these markers, the accurate subcellular localization of LHT7 will be defined. In summary, further experiments involving the identification of transgenic plants and tests on tissue-specific localization, as

well as investigations into subcellular localization through co-infiltration, are necessary to further our understanding of LHT7's role in plant immunity.

To address the second objective of this study, I generated both constitutive construct and inducible construct to investigate the role of *LHT7* in plant immunity. In future studies, the estradiol-inducible construct should be introduced into Arabidopsis via agrobacterium-mediated transformation of immature flowers. Additionally, it is crucial to transform both, overexpression constructs and estradiol-inducible constructs into the *lht7* background plants to determine if they can rescue the susceptible phenotype of the mutant.

Methods and Materials

Cloning Method

Gateway Cloning Method

Gateway Cloning is a widely used cloning technique that allows researchers to transfer DNA fragments between different plasmids by a set of recombination sequences. It can be divided into two reactions: BP reaction and LR reaction. In the BP reaction, DNA fragments can be amplified using primers that include attB sites. The PCR product is then recombined with a donor vector that contains the complementary attP sites using BP clonase. In the LR reaction, the entry clone is mixed with a destination vector that contains attR sites, and the LR clonase is used to catalyze a second recombination event. The LR reaction can simultaneously transfer the gene of interest to one or more destination vectors, making the cloning work efficiently (Katzen, 2007).
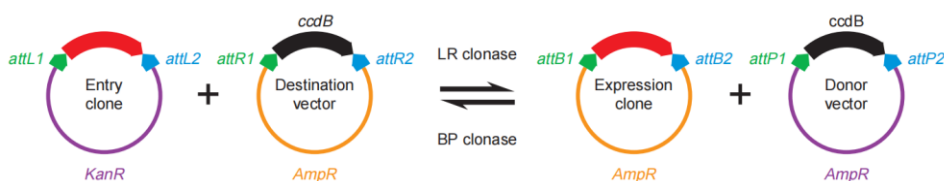

Fig 17. The Gateway reactions. The scheme shows the four types of plasmids and enzyme mixes involved in Gateway cloning reactions. Red arrows represent the fragment of interest.

One disadvantage of Gateway cloning is that long and expensive primers have to be used to get an attB-tagged PCR product. To avoid this drawback, a two-step PCR developed by *Invitrogen* is used. Amplification of PCR product using plant genomic DNA and specific primers that contain 12 nucleotides of the attB sites (Table 1). Phusion® High-Fidelity DNA Polymerases are used and the reaction components are listed below.

Component	Volume (50 µl Reaction)	Final Concentration
5X Phusion HF Buffer	10 µl	1x
10 mM dNTPs	1 µl	200 µM
attB-tagged primer F (10 µM)	2.5 µl	0.5 µM
attB-tagged primer R (10 µM)	2.5 µl	0.5 µM
Plant genomic DNA	1µl	
DMSO	1.5 µl	3 %
Phusion DNA Polymerase	0.5µl	1.0 units/50 µl PCR
Nuclease-free water	31 µl	

Thermocycling conditions for Step-1 PCR:

STEP	TEMP	TIME
Initial Denaturation	98°C	30 seconds
	98°C	5-10 seconds
35 cycles	45-72°C	10-30 seconds
	72°C	15-30 seconds per kb
Final Extension	72°C	5-10 minutes
Hold	4°C	

Take 2 µl of the PCR product to perform agarose gel electrophoresis to ensure the reaction succeeds. Using universal attB primers (Table 1) to amplify the PCR product in Step-1. The component of the Step-2 reaction is listed below.

Component	Volume (50 µl Reaction)
PCR product Step-1	10 µl
10 mM dNTPs	1µl
Universal attB1 adapter primer (10 pmol/µl)	4 µl
Universal attB2 adapter primer (10 pmol/µl)	4 µl
Phusion DNA Polymerase	1 µl
5X Phusion HF Buffer	10 µl
Nuclease-free water	20 µl

Thermocycling conditions for Step-2 PCR:

STEP	TEMP	TIME	
Denaturation	98°C	2 min	
Denaturation	98°C	30 seconds	
Annealing	45°C	30 seconds	5 cycles
Extension	72°C	15-30 seconds per kb	
Denaturation	98°C	15 seconds	
Annealing	55°C	30 seconds	15-20 cycles
Extension	72°C	15-30 seconds per kb	
Final Extension	72°C	5-10 minutes	
Hold	4°C		

Gibson Cloning Method

Gibson is a molecular cloning method that can assemble up to 15 DNA fragments in one reaction based on sequence identity. Based on this technique, the *New England BioLabs* developed *NEBuilder* (https://nebuilder.neb.com/#!/) and its correspondent kit to help researchers design primers and run the reaction. This reaction is mixed with a cocktail of three enzymes, exonuclease, DNA polymerase, and DNA ligase; along with other buffer components (Gibson et al., 2009). In this study, double digestion is used to get a linear vector. After

27

PCR amplification, DNA fragments are put together with NEBuilder® HiFi DNA Assembly master mix. Samples are incubated at 50°C for 15 minutes when 2-3 fragments are being assembled or 60 minutes when 4-6 fragments are being assembled. Transfer 2 μl reaction to NEB 5-alpha competent *E. coli* cells and culture them on the plates with the corresponding antibiotic (Fig 18) (*New England BioLabs*, https://www.neb.com).
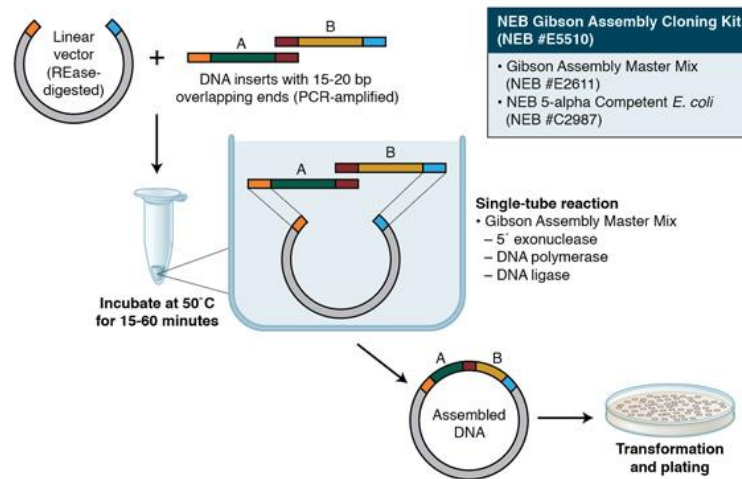

Fig 18. Gibson Assembly Workflow.

Plant material

Arabidopsis thaliana ecotype Col-0 and T-DNA insertional mutant lines, *lht7-1* (SALK_027033) and *lht7-2* (SALK_043012), which have a Col-0 background, were acquired from the ABRC at Ohio State University. The mutant lines are checked by PCR to confirm they have T-DNA insertion in the correct location. Seedlings were grown in Murashige and Skoog (MS) basal medium with 0.5 g/L MES hydrate and 0.5% sucrose and adjusted to a pH of 5.7 with KOH. Seedlings are cultured in Conviron Adaptis A1000 growth chambers (Conviron, Inc.) under 16 hours of light photoperiod, 22.5°C constant temperature, 100umol light intensity, and 80% relative humidity to prevent evaporation. Before being cultured in liquid MS medium, seeds are sterilized by using 20% bleach washed 3 times, and stored in the dark and 4°C condition for at least

two days. Plants intended for infection assays are grown in pellets (JIFFY PRODUCTS OF AMERICA) for 5 to 6 weeks under 10 hours of light photoperiod. For the initial four weeks, the plants are watered thrice a week with Hoagland solution. In the final two weeks before infection, the plants are watered thrice a week with tap water.

Agrobacterium-mediated transformation

The plants used for Agrobacterium transformation are grown in soil-filled pots under a 10-hour photoperiod with a constant temperature of 22.5°C, 100umol light intensity, and 80% relative humidity. After identifying the healthiest plants, they are thinned down to two. Tap water is used twice a week for watering before transformation, and once siliques appear, Hoagland solution water is used twice a week. When the first inflorescence grows to a height of 2.5 cm, it should be cut to encourage more inflorescence growth. The first floral dip is recommended when the inflorescence reaches a length of about 5 cm. *Agrobacterium CV3101* (Rif resistance) is used for all the transformations. The desired colony is cultured in 20 mL YEP medium with the corresponding antibiotic in a sterile 250 mL Erlenmeyer flask overnight. Cells are harvested by centrifugation in 50 mL Falcon tubes at 3750 rpm for 15 minutes. After pouring out the medium, the bacterial pellet is resuspended in 25 mL dipping solution (5% Suc, 0.04% silwet) and poured into a petri dish. The Arabidopsis inflorescences are then inverted into the solution for 10 seconds and only dipped once in each experiment. Following the dipping step, the plants are kept in a 100% humidity chamber for 24 hours before being returned to the growth chamber. The dipping step is repeated after 6 days, and a total of 3 times. Finally, mature dry seeds are collected in a tube and screened on MS agar plates with the corresponding antibiotic (Deblaere et al., 1985).

Plant Infection Assay

Use 5- to 6-week-old plants to do the bacteria infection assay. Both *Pseudomonas syringae maculicola ES4326* (*Psm*) and *Pseudomonas syringae pv tomato DC3000* (*Pst*) are used in this study. Using a sterile p200 tip, streak the Pst and Psm colonies from the stock and culture them overnight on fresh LB plates with the corresponding antibiotic. The following morning, take a small amount of inoculum from a fresh *P. syringae* plate using a sterile p200 tip and introduce it to a 50 mL conical tube containing 2 mL of liquid King's Broth medium (proteose peptone 20 g/L, K2HPO4 1.5 g/L, Glycerol 50% 10 ml/L, MgSO4 x 7H2O 1.5 g/L (6 mM final)). Grow the bacteria in a shaker at 28°C and 250 rpm for approximately 3-4 hours until the OD600 reaches 0.4-0.8. Transfer the medium to a tube and centrifuge at 6500 rpm for 3 minutes, then wash twice with water. Measure the OD value and dilute it to OD600=0.0002 with water. Inoculate four fully expanded leaves and return them to the growth chamber. After 72 hours, collect the infected leaves and punch them to obtain leaf discs. Add 400 μl sterile H2O and 1 steel bead to each tube and place them in the tissue lyser. Shake at 25 shakes/s for 10 minutes and then dilute the lysates in a series of 10 times. Transfer 5 μl of each dilution to LB plates with the corresponding antibiotic and culture overnight in a 28°C chamber. Finally, count the CFU.

Fluorescent Imaging

One-week-old seedlings of *35S::gDNA of LHT7 –mCherry* transgenic line are used for imaging. Grow sterile seeds in a 12-well plate with liquid MS medium. Leica STELLARIS 8 Confocal system is used for fluorescent imaging. The mCherry is visualized by excitation at 587nm and emission from 595-620nm (Shu et al., 2006).

RNA work and gene expression analysis

Seedlings and plant leaves were flashed frozen in liquid nitrogen and used the Trizol-RNA extraction protocol (Invitrogen). Treat 10 µg RNA with RQ1 RNase-free DNAse-I from Promega to remove genomic DNA. Use PR1-U1 and PR1-L1 primers (Table 1) to ensure that DNAse-I completely clean the DNA contamination. To synthesize first-strand cDNA, begin by combining 2 µg RNA and 2 µL of random decamers in a 200 µL PCR tube. Adjust the reaction volume to 15 µL using RNAse-free water and incubate the mixture at 70°C for 5 minutes to eliminate any secondary structure in the RNA. Immediately place the reaction on ice to prevent the reformation of the secondary structure. Next, prepare the master mix by combining 5 µL of 5X M-MLV Buffer (Promega), 2 µL of 10 mM 4dNTPs, 1 µL of RNA-inhibitor, 1 µL of M-MLV RT (200U), and 1 µL of water. Add 10 µL of the master mix to each sample and mix thoroughly by flicking the tube. Incubate the tubes at room temperature for 3 minutes and then transfer them to a PCR machine at 37°C for 60 minutes for cDNA synthesis.

For qPCR, prepare the master mix by combining 10 µL of SYBR-green and 7 µL of water. Aliquot 17 µL of the master mix to different cDNA templates (1 µL). To the control group, add 2 µL of 5 µM ACT2-U4 and ACT2-L4 primers (Table 1). To the experiment group, add 2 µL of 5 µM qLHT7-F2 and qLHT7-R2 primers (Table 1). Transfer the reactions to the 7500 Real-Time PCR System and run the qPCR assay. Normalize the gene expression data to Actin2 expression.

Table 1. List of primers sequences in this study

Primer Name	Sequence (5'-3')
LHT7_pF	GGGGACAAGTTTGTACAAAAAAGCAGGCTTAATGTCTATAGCATT GGGAAACTTATTTGATTTGG
LHT7_pR	GGGGACCACTTTGTACAAGAAAGCTGGGTTTTAGGGTCTGAAGA AGTTAGCATGCAAAC
LHT7_pRX	GGGGACCACTTTGTACAAGAAAGCTGGGTTTCCGGGTCTGAAGA AGTTAGCATGCAAAC
pLHT7_pF	GGGGACAAGTTTGTACAAAAAAGCAGGCTTAACCTAGCTGATGTA ACTATTTG
pLHT7_pR	GGGGACCACTTTGTACAAGAAAGCTGGGTTAAATGTTTACTCTGC TTTCATTG
qLHT7-F2	GGCTGCCGATCACAGAATCA
qLHT7-R2	ACAAGAAGCCACGTCGTGTA
SALK_043012-L	TTCTAACGATTGCAAGGATGC
SALK_043012-R	ACAGCGCCACTTACTTCAGTG
Lht7-detect-L	GTTGCCCACGGGACCT
lht7-2-detect-l	GGTTCTCCTTTATTTATGTCACCAG
gLHT7-F1	AAAAAGCAGGCTTCCTTGCGTTGACCAAAACATC
gLHT7-R1	AGAAAGCTGGGTTCCCGCAACTTTCTTCACTGT
gLHT7-R2	AGAAAGCTGGGTTCATCCGGTCAGGTAAACCAT
PG-LHT7-F1	AAAAAGCAGGCTTCAGCTGGTCATCATCAACTCG
PG-LHT7-F2	AAAAAGCAGGCTTCCCAAACAACAACTTCGGACGT
PG-LHT7-R1	AGAAAGCTGGGTTGGGTCTGAAGAAGTTAGCATGC
LHT7-CDS-Seq-F	CGTTGATCGGTGCTTTTATGGG
LHT7-CDS-Seq-R	CCATTGTAGCGTACGAGACAC
mcherry-AscI-F	GCATGTGGCGCGCCATGGTGAGCAAGGGCGAGG
mcherry-PacI-R	CGACTGTTAATTAATTACTTGTACAGCTCGTCCATGC

gLHT7-seq	GGGACTACTAACATGTTC
eGFP-L	ACAAGTTCAGCGTGTCCG
eGFP-R	TCTCGTTGGGGTCTTTGC
PG_LHT7_Fwd	AAAAAGCAGGCTGCACCTAGCTGATGTAACTATTTGC
PG_LHT7_Rev	AGAAAGCTGGGTCGGGTCTGAAGAAGTTAGCATGC
mcherry_fwd_update	CTTCAGACCCATGGTGAGCAAGGGCGAG
mcherry_rev	GCCTGGATCGACTAGTTAATTTACTTGTACAGCTCGTCCATG
Fwd-LHT7-CDS-XhoI	GATCCTCTCGAGATGTCTATAGCATTGGGAAACTTATTTGAT TTGG
Rev-LHT7-CDS-SpeI	CCGCACACTAGTTTAGGGTCTGAAGAAGTTAGCATGCAAAC
gLHT7-R1 (two-step)	CCCGCAACTTTCTTCACTGT
gLHT7-R2 (two-step)	CATCCGGTCAGGTAAACCAT
gLHT7-F1 (two-step)	CTTGCGTTGACCAAAACATC
mcherry-L	ATGGTGAGCAAGGGCGAGG
mcherry-R	TTACTTGTACAGCTCGTCCATGC
PG of LHT7-seq1	CTAAATCATCATTATGCTG
PG of LHT7-seq2	CGCTGAGAGAAGCACCTAG
PG of LHT7-seq3	GAGCTATCAATCCAATAGCG
PG of LHT7-seq4	GTTATTACCATCCGAGTG
PG of LHT7-seq5	GGTCAACGCAAGGGTCAAC
PG of LHT7-seq6	CTATCTATGTTAGAACTTAC
PG of LHT7-seq7	GGTTCCGTTTCTTTATGTGATG
mcherry_fwd	CCGGTTAAATATGGTGAGCAAGGGCGAG
GB_gDNAx_fwd	AGTCGACTCTAGCCTCGAGGATGTCTATAGCATTGGGAAAC
GB_gDNAx_rev	TGCTCACCATGGGTCTGAAGAAGTTAGCATG
plasmid-14_detect	GACCGGCAACAGGATTC
pLHT7_seq1	CGGACATTATCGTCCTG
pLHT7_seq2	GGTCTCACATAACTAGAG

GUS_fwd_p17	TTTGTATACAATGTTACGTCCTGTAGAAAC
GUS_rev_p17	GAACATCGTATGGGTACATATCAGATCTGTTGTTTG
pLHT7_Gus_fwd	CCAGTCACTATGGCGGCCCCGCCATCTAGTGTGAAT
pLHT7_Gus_rev	GACGTAACATTGTATACAAAATAAACTTTATTTTCC
Seq-gLHT7	CGATACCGTTTCTGATGTTG
pLHT7_fwd_update_XhoI	CCAGTCACTATGGCGGCCCCGCCATCTAGTGTGAATA TCCG
pLHT7_rev_C	CTATAGACATTGTATACAAAATAAACTTTATTTTCCTCT AAC
gLHT7x_fwd_C	TTTGTATACAATGTCTATAGCATTGGGAAAC
gLHT7x_rev_C	TGCTCACCATGGGTCTGAAGAAGTTAGCATG
mCherry_fwd_C	CTTCAGACCCATGGTGAGCAAGGGCGAG
mCherry_rev_C	GAACATCGTATGGGTACATATTACTTGTACAGCTCGTC CATG
pLHT7_rev_N	TGCTCACCATTGTATACAAAATAAACTTTATTTTCCTCT AAC
mCherry_xstop_fwd_N	TTTGTATACAATGGTGAGCAAGGGCGAG
mCherry_xstop_rev_N	CTATAGACATCTTGTACAGCTCGTCCATG
gLHT7_3UTR_stop_fwd_N	GCTGTACAAGATGTCTATAGCATTGGGAAAC
gLHT7_3UTR_stop_rev_N	GAACATCGTATGGGTACATATCAAAATGAACAGCATAA TGATG
pLHT7_seq	GGCTTGAAGCTAAACTTG
GUS_seq1	GGAATGGTGATTACCGACG
GUS_seq2	GAGCTGATAGCGCGTGAC

Reference

Agorsor, I. D., Kagel, B. T., & Danna, C. H. (2023). The Arabidopsis LHT1 Amino Acid Transporter Contributes to Pseudomonas simiae-Mediated Plant Growth Promotion by Modulating Bacterial Metabolism in the Rhizosphere. *Plants*, 12(2), 371.

Anderson, J. C., Wan, Y., Kim, Y. M., Pasa-Tolic, L., Metz, T. O., & Peck, S. C. (2014). Decreased abundance of type III secretion system-inducing signals in Arabidopsis mkp1 enhances resistance against Pseudomonas syringae. Proceedings of the National *Academy of Sciences*, 111 (18), 6846-6851.

Aung, K., Kim, P., Li, Z., Joe, A., Kvitko, B., Alfano, J.R., He, S.Y., 2020. Pathogenic Bacteria Target Plant Plasmodesmata to Colonize and Invade Surrounding Tissues. *Plant Cell* 32, 595–611. https://doi.org/10.1105/tpc.19.00707

Bender CL, Alarcon-Chaidez F, Gross DC. 1999. Pseudomonas syringae phytotoxins: mode of action, regulation, and biosynthesis by peptide and polyketide synthetases. *Microbiol. Mol. Biol. Rev.* 63:266–92.

Blanco, C., Ritzenthaler, P., & Mata-Gilsinger, M. (1982). Cloning and endonuclease restriction analysis of uidA and uidR genes in Escherichia coli K-12: determination of transcription direction for the uidA gene. *Journal of Bacteriology*, 149 (2), 587–594. https://doi.org/10.1128/jb.149.2.587-594.1982

Brooks DM, Bender CL, Kunkel BN. 2005. The Pseudomonas syringae phytotoxin coronatine promotes virulence by overcoming salicylic acid–dependent defences in *Arabidopsis thaliana. Mol. Plant Pathol*. 6:629–39.

Brooks DM, Hernandez-Guzman G, Kloek AP, Alarcon-Chaidez F, Sreedharan A, et al. 2004. Identification and characterization of a well-defined series

of coronatine biosynthetic mutants of *Pseudomonas syringae pv. tomato DC3000. Mol. Plant-Microbe Interact.* 17:162–74.

Buell, C. R., Joardar, V., Lindeberg, M., Selengut, J., Paulsen, I. T., Gwinn, M. L., ... & Collmer, A. (2003). The complete genome sequence of the Arabidopsis and tomato pathogen Pseudomonas syringae pv. tomato DC3000. *Proceedings of the National Academy of Sciences*, 100(18), 10181-10186.

Buttner D, He SY. 2009. Type III protein secretion in plant pathogenic bacteria. *Plant Physiol.* 150:1656–64.

Chakraborty, S., & Newton, A. C. (2011). Climate change, plant diseases and food security: an overview. *Plant pathology*, 60 (1), 2-14.

Chatnaparat, T., Li, Z., Korban, S. S., & Zhao, Y. (2015). The stringent response mediated by (p) ppGpp is required for virulence of Pseudomonas syringae pv. tomato and its survival on tomato. *Molecular Plant-Microbe Interactions*, 28 (7), 776-789.

Chen, L., Ortiz-Lopez, A., Jung, A., & Bush, D. R. (2001). ANT1, an aromatic and neutral amino acid transporter in Arabidopsis. *Plant Physiology*, 125(4), 1813-1820.

Chinchilla, D., Bauer, Z., Regenass, M., Boller, T., & Felix, G. (2006). The Arabidopsis receptor kinase FLS2 binds flg22 and determines the specificity of flagellin perception. *The Plant Cell*, 18(2), 465-476.

Clough, S. J., & Bent, A. F. (1998). Floral dip: a simplified method for Agrobacterium‐mediated transformation of Arabidopsis thaliana. *The plant journal*, 16(6), 735-743.

Cunnac S, Lindeberg M, Collmer A. 2009. Pseudomonas syringae type III secretion system effectors: repertoires in search of functions. *Curr. Opin. Microbiol.* 12:53–60.

Deblaere, R., Bytebier, B., De Greve, H., Deboeck, F., Schell, J., Van Montagu, M., & Leemans, J. (1985). Efficient octopine Ti plasmid-derived vectors for Agrobacterium-mediated gene transfer to plants. Nucleic acids research, 13(13), 4777-4788.

Dodds, P. N., & Rathjen, J. P. (2010). Plant immunity: towards an integrated view of plant–pathogen interactions. *Nature Reviews Genetics*, 11 (8), 539-548.

Engler, Carola; Marillonnet, Sylvestre (2014-01-01). "Golden Gate cloning". Methods in Molecular Biology. 1116: 119–131. doi:10.1007/978-1-62703-764-8_9. ISBN 978-1-62703-763-1. ISSN 1940-6029. PMID 24395361.

Frommer, W. B., Hummel, S., & Riesmeier, J. W. (1993). Expression cloning in yeast of a cDNA encoding a broad specificity amino acid permease from Arabidopsis thaliana. Proceedings of the National Academy of Sciences, 90(13), 5944-5948.

Frommer, W. B., Hummel, S., Unseld, M., & Ninnemann, O. (1995). Seed and vascular expression of a high-affinity transporter for cationic amino acids in Arabidopsis. *Proceedings of the National Academy of Sciences*, 92(26), 12036-12040.

Galan JE, Collmer A. 1999. Type III secretion machines: bacterial devices for protein delivery into host cells. *Science* 284:1322–28.

Gibson, D. G., Young, L., Chuang, R. Y., Venter, J. C., Hutchison III, C. A., & Smith, H. O. (2009). Enzymatic assembly of DNA molecules up to several hundred kilobases. Nature methods, 6(5), 343-345.

Hirner, A., Ladwig, F., Stransky, H., Okumoto, S., Keinath, M., Harms, A., ... & Koch, W. (2006). Arabidopsis LHT1 is a high-affinity transporter for cellular amino acid uptake in both root epidermis and leaf mesophyll. The Plant Cell, 18(8), 1931-1946.

Hsu, L. C., Chiou, T. J., Chen, L., & Bush, D. R. (1993). Cloning a plant amino acid transporter by functional complementation of a yeast amino acid transport mutant. *Proceedings of the National Academy of Sciences*, 90(16), 7441-7445.

Jefferson, R. A., Burgess, S. M., & Hirsh, D. (1986). beta-Glucuronidase from Escherichia coli as a gene-fusion marker. *Proceedings of the National Academy of Sciences of the United States of America*, 83 (22), 8447–8451. https://doi.org/10.1073/pnas.83.22.8447

Jones, J. D., & Dangl, J. L. (2006). The plant immune system. *Nature*, 444 (7117), 323-329.

Jones, J.D.G., Dangl, J.L., 2006. The plant immune system. Nature 444, 323–329. https://doi.org/10.1038/nature05286

Kapila, J., De Rycke, R., Van Montagu, M., & Angenon, G. (1997). An Agrobacterium-mediated transient gene expression system for intact leaves. *Plant science,* 122(1), 101-108.

Katzen F. (2007). Gateway(®) recombinational cloning: a biological operating system. Expert opinion on drug discovery, 2(4), 571–589. https://doi.org/10.1517/17460441.2.4.571

Koch, W., Kwart, M., Laubner, M., Heineke, D., Stransky, H., Frommer, W. B., & Tegeder, M. (2003). Reduced amino acid content in transgenic potato tubers due to antisense inhibition of the leaf H+/amino acid symporter StAAP1. *The Plant Journal,* 33(2), 211-220.

Krämer U. (2015). Planting molecular functions in an ecological context with Arabidopsis thaliana. eLife, 4, e06100. https://doi.org/10.7554/eLife.06100.

Lee, Y. H., Foster, J., Chen, J., Voll, L. M., Weber, A. P., & Tegeder, M. (2007). AAP1 transports uncharged amino acids into roots of Arabidopsis. *The Plant Journal*, 50(2), 305-319.

Lindeberg M, Myers CR, Collmer A, Schneider DJ. 2008. Roadmap to new virulence determinants in Pseudomonas syringae: insights from comparative genomics and genome organization. *Mol. Plant-Microbe Interact.* 21:685–700.

Melotto, M., Underwood, W., & He, S. Y. (2008). Role of stomata in plant innate immunity and foliar bacterial diseases. *Annual Review of Phytopathology*, 46, 101.

Näsholm, T., Kielland, K., & Ganeteg, U. (2009). Uptake of organic nitrogen by plants. *New phytologist*, 182(1), 31-48.

Nelson, B. K., Cai, X., & Nebenführ, A. (2007). A multicolored set of in vivo organelle markers for co‐localization studies in Arabidopsis and other plants. *The Plant Journal*, 51(6), 1126-1136.

Ortiz-Lopez, A., Chang, H. C., & Bush, D. R. (2000). Amino acid transporters in plants. *Biochimica et Biophysica Acta (BBA)-Biomembranes*, 1465 (1-2), 275-280.

Perchlik, M., Foster, J., & Tegeder, M. (2014). Different and overlapping functions of Arabidopsis LHT6 and AAP1 transporters in root amino acid uptake. *Journal of experimental botany*, 65(18), 5193-5204.

Pruitt, R. N., Gust, A. A., & Nürnberger, T. (2021). Plant immunity unified. *Nature plants*, 7 (4), 382-383.

Schwacke, R., Schneider, A., van der Graaff, E., Fischer, K., Catoni, E., Desimone, M., ... & Kunze, R. (2003). ARAMEMNON, a novel database for Arabidopsis integral membrane proteins. *Plant physiology,* 131(1), 16-26.

Shu, X., Shaner, N. C., Yarbrough, C. A., Tsien, R. Y., & Remington, S. J. (2006). Novel chromophores and buried charges control color in mFruits. *Biochemistry*, 45(32), 9639-9647.

Sonawala, U., Dinkeloo, K., Danna, C. H., McDowell, J. M., & Pilot, G. (2018). Functional linkages between amino acid transporters and plant responses to pathogens. *Plant Science*, 277, 79-88.

Svennerstam, H., Jämtgård, S., Ahmad, I., Huss‐Danell, K., Näsholm, T., & Ganeteg, U. (2011). Transporters in Arabidopsis roots mediating uptake of amino acids at naturally occurring concentrations. *New Phytologist,* 191(2), 459-467.

Tabuchi, S., Ito, J., Adachi, T., Ishida, H., Hata, Y., Okazaki, F., Tanaka, T., Ogino, C., & Kondo, A. (2010). Display of both N- and C-terminal target fusion proteins on the Aspergillus oryzae cell surface using a chitin-binding module. Applied microbiology and biotechnology, 87(5), 1783–1789. https://doi.org/10.1007/s00253-010-2664-6.

Tang X, Xiao Y, Zhou JM. 2006. Regulation of the type III secretion system in phytopathogenic bacteria. Mol. *Plant-Microbe Interact*. 19:1159–66.

Tegeder, M. (2014). Transporters involved in source to sink partitioning of amino acids and ureides: opportunities for crop improvement. *Journal of Experimental Botany*, 65(7), 1865-1878.

Tegeder, M., & Masclaux‐Daubresse, C. (2018). Source and sink mechanisms of nitrogen transport and use. *New Phytologist*, 217 (1), 35-53.

Tegeder, M., & Ward, J. M. (2012). Molecular evolution of plant AAP and LHT amino acid transporters. *Frontiers in Plant Science*, 3, 21.

Weber, E., Engler, C., Gruetzner, R., Werner, S., & Marillonnet, S. (2011). A modular cloning system for standardized assembly of multigene constructs. PloS one, 6(2), e16765.

Wildermuth, M. C., Dewdney, J., Wu, G., & Ausubel, F. M. (2001). Isochorismate synthase is required to synthesize salicylic acid for plant defence. *Nature*, 414(6863), 562-565.

Xin, X. F., & He, S. Y. (2013). Pseudomonas syringae pv. tomato DC3000: a model pathogen for probing disease susceptibility and hormone signaling in plants. *Annual review of phytopathology*, 51, 473-498.

Yang, G., Wei, Q., Huang, H., & Xia, J. (2020). Amino acid transporters in plant cells: A brief review. *Plants,* 9(8), 967.

Zhang, X., Khadka, P., Puchalski, P., Leehan, J. D., Rossi, F. R., Okumoto, S., ... & Danna, C. H. (2022). MAMP-elicited changes in amino acid transport activity contribute to restricting bacterial growth. *Plant Physiology*.

Zhang, X., Tubergen, P. J., Agorsor, I. D., Khadka, P., Tembe, C., Denbow, C., ... & Danna, C. H. (2023). Elicitor-induced plant immunity relies on amino acids accumulation to delay the onset of bacterial virulence. *Plant Physiology*, kiad048.